Cavity-involved plasmonic metamaterial for optical polarization conversion

T. Li,[a] S. M. Wang, J. X. Cao, H. Liu, and S. N. Zhu

National Laboratory of Solid State Microstructures, Department of Material Science and Engineering, Department of Physics, Nanjing University, Nanjing 210093, People's Republic of China

We experimentally demonstrate a plasmonic assisted Fabry–Perot cavity in a metal/insulator/metal trilayer structure with L-shaped hole arrays inside, which significantly contribute to the mechanism to realize a nearly complete polarization conversion (=0.93) in optical transmissions at near-infrared wavelength. This interesting property is found arising from an overlap of the cavity and plasmonic modes in two orthogonal polarization states. This discovered physics remarkably endows this plasmonic metamaterial with good optical performance and looser fabrication requirement, not only indicating practical applications but also providing fruitful inspirations in future nanophotonic designs. © *2010 American Institute of Physics.* [doi:10.1063/1.3533912]

Manipulating the state of optical polarization (SOP) is always a fundamental desire for people to fully control light. In recent years, using metamaterials to produce proper electromagnetic responses to achieve giant optical gyrotropy other than conventional methods (e.g., birefringence[1]) has arrested increasing attentions due to their scientific novelty.[2,3] Remarkable progresses have been made based on particular designs, such as sculptured helical[4–6] and coupled planar structures.[7–10] However, most of these approaches usually require high fabrication techniques especially for those working at optical frequencies. Moreover, complicated technical processes always bring large optical loss and result in low working efficiency. In our previous work, we demonstrated a single layer plasmonic structure containing L-shaped holes that can rotate the polarization to 45°.[11] Like the double fishnet structure,[12–14] it is reasonable to extend the single layer to metal/insulator/metal trilayer. Coupling effect may be expected in small insulator spacer case as well. However, if we go much farther to construct a cavity by extending the insulator layer thickness, this system will be endowed with more physics much different from the coupled one. As for the optical activity, polarization conversion is an important function. In principle, it requires material to have two eigenmodes with 180° phase difference at the same frequency in two orthogonal polarization states. Introducing a cavity in the L-shaped hole system does provide a further degree to modulate the eigenmodes that will possibly satisfy the condition for a complete polarization conversion.

In this letter, we combine experimental and theoretical efforts to demonstrate a cavity-involved plasmonic metamaterial, in which a nearly complete polarization conversion is realized in transmissions for certain linearly polarized light. Different from previous helix or coupling induced gyrotropy, this strong optical activity arises from an overlap of Fabry–Perot (FP) resonance and plasmonic mode in two orthogonal polarizations. Thanks to simple planar design and uncoupled nature, this structure exhibits high manufacturing tolerance. Moreover, this effect is assisted by the plasmonic induced extraordinary transmission,[15,16] and exhibits a high working efficiency.

Figures 1(a) and 1(b) schematically depict the proposed structure illuminated by a linearly polarized light, which is likely to convert the polarization completely to its orthogonal state after transmission. Here, the metal is defined as silver and the dielectric spacer is SiO_2. For experiments we perform three steps to fabricate the samples: (i) a first deposition of silver film on the quartz substrate by sputtering and followed with a milling by the focus ion beam (FIB) (FEI Co., USA); (ii) a second deposition of SiO_2 film; (iii) a third deposition of silver film, followed with a second FIB milling. It should be mentioned that no precise alignment process such as Refs. 10 and 17 is adopted in this three-step procedure. After characterizing a series of samples carefully, we choose an appropriate sample with the best performance for detailed illustrations, whose geometrical parameters are p =600 nm, a=315 nm, and b=150 nm. The thickness of silver and SiO_2 spacer are characterized of about 45 and 370 nm, respectively. This sample contains 81×81 units in total, covering an area about 49×49 μm^2. Because it lacks a special alignment process, the accurate positions of L-shaped holes in two metal layers are not exactly aligned, revealing a little bit of corrugations in the top view of sample [see Fig. 1(c)]. We will specifically discuss about these discrepancies later.

Polarization resolved spectral transmittances are elaborately analyzed by a homebuilt optical setting. A polarized white light from a halogen lamp and through a Glan–
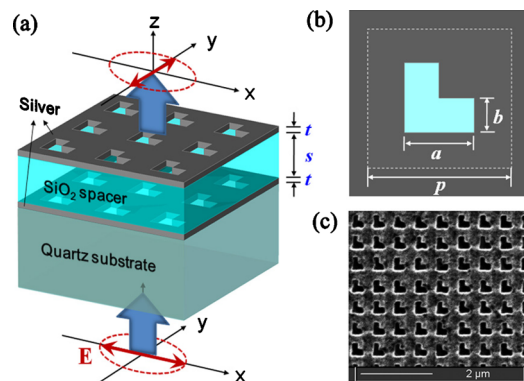

FIG. 1. (Color online) (a) Schematic of proposed structure under the illumination of a linearly polarized light; (b) unit cell of the structure; (c) FIB image of the top view of the fabricated sample.

[a]Author to whom correspondence should be addressed. Electronic mail: taoli@nju.edu.cn.
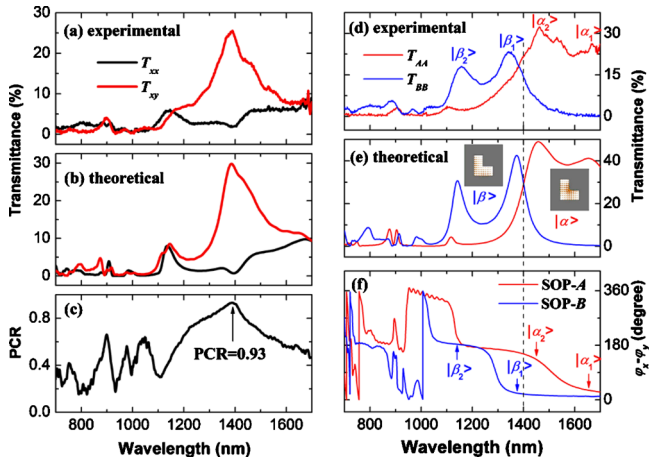
FIG. 2. (Color online) (a) Experimental and (b) theoretical transmission spectra in two orthogonal polarization states with x-polarization incidence; (c) PCR retrieved from the experimental data; (d) experimental and (e) theoretical transmission spectra for two major polarization states. Inset images in (e) are the simulated in-plane electric field distributions for the $|\alpha_i\rangle$ and $|\beta_i\rangle$ modes; (f) phase differences ($\varphi_x - \varphi_y$) of these two major SOPs as functions of the wavelength.

Thomson prism illuminates normally onto the sample. Optical transmission with the polarization checked by another prism is collected by an optical spectrum analyzer via a fiber coupler. By tuning prisms, we can obtain the transmittance in any polarization states. We first investigate the case of incidence with x-polarization, which is possibly considered the largest optical rotation. Figure 2(a) shows the polarized transmittances both from the original x-polarization (T_{xx}) and its orthogonal y-polarization (T_{xy}) (T_{ij} denotes j-polarized transmittance from i-polarized incidence). A remarkable polarization conversion is revealed as a transmission peak in T_{xy} at about 1400 nm with a dip in T_{xx}, indicating an energy transferring from original polarization state to the orthogonal one with an almost 90° rotation. Although the transmittance (T_{xy}) is about 25%, it already exceeds the unit as normalized to the equivalent holes area attributing to the plasmonic induced enhanced optical transmission. Honestly, we admit this absolute transmittance cannot ultimately reach 100% in such a lossy plasmonic system, though it may be further improved by optimizing the design and fabrication. Nevertheless, this shortcoming may be overcome by adopting gain medium (e.g., replace the middle layer by quantum dots included active polymer[18]).

Afterward, we performed a set of finite integration calculations using a commercial software package (CST MICROWAVE STUDIO), where the dielectric function of silver is defined by Drude mode with $\omega_p = 1.37 \times 10^{16}$ rad/s and $\gamma = 8.5 \times 10^{13}$ rad/s.[11] Periodic boundary conditions are set in x and y directions representing a periodical structure, and open (perfectly matching layer) boundary is defined in z direction for the light incidence and transmission. Electric probes along x and y directions are located 5 μm behind the sample to detect the transmitted field for different polarizations. The refractive indices of the SiO_2 spacer and quartz substrate are both set as 1.47. The corresponding calculation results of the polarized transmittances are shown in Fig. 2(b), where well-reproduced spectra show good agreements with the experiment results. As well as Ref. 19, we introduce a polarization conversion rate (PCR) to evaluate its performance, which is defined as PCR $= T_{xy}/(T_{xx}+T_{xy})$. It is clearly
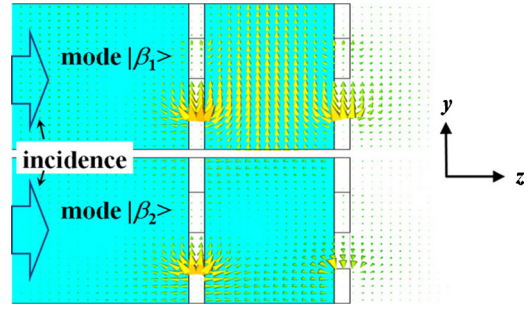

FIG. 3. (Color online) Electric field distributions in y-z plane for the modes $|\beta 1\rangle$ and $|\beta 2\rangle$.

found the maximum PCR reaches a high value of 0.93 at about 1400 nm as shown in Fig. 2(c).

To verify our preliminary ideas as well as to find the physics origin of this polarization conversion, we analyze another two cases of incidence of polarization of 45° and −45°, which are considered as two major states and defined as SOP-A and SOP-B, respectively. Figure 2(d) shows two transmission spectra defined as T_{AA} and T_{BB}. Very weak transmittances observed in their orthogonal states T_{AB} and T_{BA} (not shown) indicate no polarization conversion occurs. The transmission peaks in Fig. 2(d) really manifest these eigenmodes marked as $|\alpha_1\rangle|\alpha_2\rangle$ and $|\beta_1\rangle|\beta_2\rangle$ for two polarization states, respectively, in good agreement with the calculations [see Fig. 2(e)]. Judging from the electric field distribution of these eigenmodes as the inset images in Fig. 2(e) show, we would presumably consider that the polarization conversion occurred at about 1400 nm for the incidence of SOP-x may be related with the overlap of the eigenmodes of $|\alpha_2\rangle$ and $|\beta_1\rangle$. Detailed comparison of the phase difference from the probe detections [see Fig. 2(f)] confirms our assumption, where an about 135° phase difference is exhibited. While not a complete 180° reversal, it basically meets the condition for polarization conversion. Thereafter, we get a clear picture of the case of SOP-x incident, that the x-polarized electric field has two orthogonal components (SOP-A and B), which will be reassembled with different modulations in their phases when light passes through the sample. Owing to the overlap of two eigenstates of $|\alpha_2\rangle$ and $|\beta_1\rangle$, a nearly half-period phase change occurs between these two field components, therefore resulting in an almost 90° polarization rotation after the recombination of electric field components in transmissions.

In addition, we depict the electric field distributions in y-z plane of the modes $|\beta_1\rangle$ and $|\beta_2\rangle$, for example, in Fig. 3. In-phase and antiphase resonances within the holes of two metal layers are clearly manifested according to these two modes, respectively. Nevertheless, these two modes are not as same as the split ones of the coupled systems (e.g., the fishnet structure[17,20]) because of the large distance (370 nm) between two metal layers. As revealed in Fig. 3, the electric field for mode $|\beta_1\rangle$ is not merely concentrated in the holes of metal layers but spreads strongly into the spacer layer, indicating to be a cavity mode. As for mode $|\beta_2\rangle$, the enhanced field inside the metal holes implies it to maintain a plasmonic mode. Similar features are revealed in the $|\alpha_1\rangle$ and $|\alpha_2\rangle$ as well (not shown).

Next, we perform detailed calculations by varying the SiO_2 spacer thickness to make a further study of the cavity modes. Here, the thicknesses are set normalized to the in-
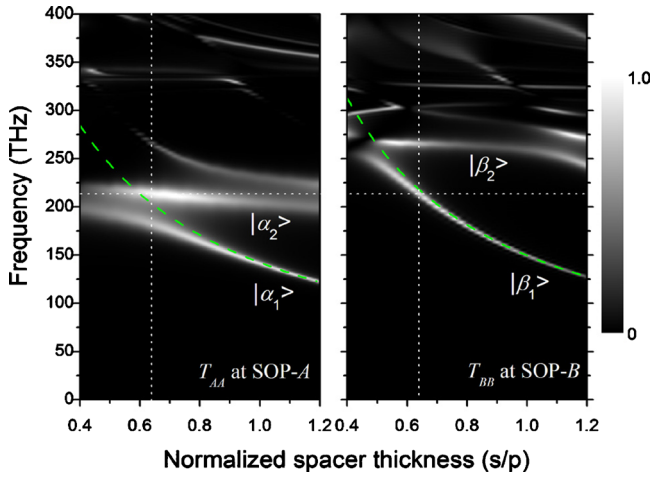
FIG. 4. (Color online) Grey scale transmittance maps in two major polarization states (T_{AA} and T_{BB}) with respect to the frequency and normalized SiO$_2$ spacer thickness (s/p). Dashed curves are the fitted curves according to Eq. (1) with $m=0$. Dotted lines are guides for the overlapping of two strong modes of $|\alpha_2\rangle$ and $|\beta_1\rangle$.

plane period (s/p) that ranges from 0.4 to 1.2. Figure 4 exhibits multiple modes revealed as the gray scale transmission maps with respect to the frequency and spacer thickness (s/p) for two major polarization states. It is evident that the lowest mode $|\alpha_1\rangle(|\beta_1\rangle)$ is rather different to the higher modes $|\alpha_2\rangle(|\beta_2\rangle)$ showing a strong dependence on the spacer thickness. This mode very likely belongs to a FP cavity mode, whose resonant condition can be described as

$$\frac{2\pi n L_{FP}}{\lambda} + \varphi_{res}(|\text{mode}\rangle) = m\pi, \qquad (1)$$

where $L_{FP} \approx s+2t$ is the effective cavity length and φ_{res} is the total phase change dominated by the plasmonic resonances. According to field distributions in Fig. 3, this lowest mode $|\beta_1\rangle$ should correspond to $m=0$ in Eq. (1). This means the plasmonic resonance in the metal layer brings a counteraction to the phase evolution from the cavity length. With this condition we try to fit the calculated FP cavity modes ($|\alpha_1\rangle$ and $|\beta_1\rangle$) by the simulated data from the case of $s/p=1.2$, shown as the green dashed curves in Fig. 4. Although discrepancies emerge in small s/p region, the thickness dependent tendency is undoubtedly in good agreement and confirms the characteristic of the FP cavity modes.[21]

As for the higher mode $|\alpha_2\rangle(|\beta_2\rangle)$, it appears as a flat line and is independent to the spacer thickness.[21] By analyzing the field distribution in Fig. 3, we contribute it to a pure plasmonic resonance mode, where enhanced field mainly concentrates in the first metal-layer holes. Actually, the antiphased resonance in the second layer holes is rather weaker than the first one and may be regarded as a forced oscillation, which also can be strong if the propagating wave happens to be phase matched. Fortunately, our sample does construct a strong antiphased plasmonic mode $|\alpha_2\rangle$ in SOP-*A* overlapped with the strong in-phase cavity mode $|\beta_1\rangle$ in SOP-*B* at the place of $s/p=0.63$ and $f=214$ THz, indicated by crossovers from the guidelines (white dotted) in Fig. 4.

It is important to point out that whatever mode considered here is not a coupled one, which depends little on the alignment of the hole arrays in two metal layers. It well explains why we can achieve such a good optical performance without precise alignment in sample fabrication. Fur-

ther calculations show that this optical polarization conversion effect is almost unaffected by the deviations of hole locations (not shown). Therefore, in-plane discrepancies introduced in FIB fabrications do not influence its optical performance greatly, which rightly shows the great advantages of this design that has considerable high manufacturing tolerance.

In summary, we proposed and fabricated a trilayer plasmonic structure to realize an almost complete and efficient polarization conversion. A maximum PCR value of about 93% is experimentally achieved at 1400 nm with a relative high transmittance. Detailed analyses indicate that the constructed FP cavity modes cooperate with the hybrid plasmonic modes and lead to an overlap between two major polarization states, which appropriately modify the phase evolutions to realize a complete polarization conversion. The revealed mechanism is substantially different from the previous coupled system and exhibits great advantages in fabrications. It will not only promise practical applications in polarization control of light, but it also may create inspirations in future designs for plasmonic materials.

[1] M. Born and E. Wolf, *Principles of Optics* (Cambridge University Press, Cambridge, 1999).
[2] J. Pendry, Science **306**, 1353 (2004).
[3] M. Wegener and S. Linden, Phys. **2**, 3 (2009).
[4] M. Thiel, M. Decker, M. Deubel, M. Wegener, S. Linden, and G. von Freymann, Adv. Mater. **19**, 207 (2007).
[5] J. K. Gansel, M. Thiel, M. S. Rill, M. Decker, K. Bade, V. Saile, G. von Freymann, S. Linden, and M. Wegener, Science **325**, 1513 (2009).
[6] S. Zhang, Y. S. Park, J. Li, X. C. Lu, W. L. Zhang, and X. Zhang, Phys. Rev. Lett. **102**, 023901 (2009).
[7] A. V. Rogacheva, V. A. Fedotov, A. S. Schwanecke, and N. I. Zheludev, Phys. Rev. Lett. **97**, 177401 (2006).
[8] M. Decker, M. W. Klein, M. Wegener, and S. Linden, Opt. Lett. **32**, 856 (2007).
[9] E. Plum, J. Zhou, J. Dong, V. A. Fedotov, T. Koschny, C. M. Soukoulis, and N. I. Zheludev, Phys. Rev. B **79**, 035407 (2009).
[10] N. Liu, H. Liu, S. N. Zhu, and H. Giessen, Nat. Photonics **3**, 157 (2009).
[11] T. Li, H. Liu, S. M. Wang, X. G. Yin, F. M. Wang, S. N. Zhu, and X. Zhang, Appl. Phys. Lett. **93**, 021110 (2008).
[12] S. Zhang, W. J. Fan, N. C. Panoiu, K. J. Malloy, R. M. Osgood, and S. R. J. Brueck, Phys. Rev. Lett. **95**, 137404 (2005).
[13] G. Dolling, C. Enkrich, M. Wegener, C. M. Soukoulis, and S. Linden, Science **312**, 892 (2006).
[14] T. Li, J. Q. Li, F. M. Wang, Q. J. Wang, H. Liu, S. N. Zhu, and Y. Y. Zhu, Appl. Phys. Lett. **90**, 251112 (2007).
[15] T. W. Ebbesen, H. J. Lezec, H. F. Ghaemi, T. Thio, and P. A. Wolff, Nature (London) **391**, 667 (1998).
[16] K. J. Klein Koerkamp, S. Enoch, F. B. Segerink, N. F. van Hulst, and L. Kuipers, Phys. Rev. Lett. **92**, 183901 (2004).
[17] N. Liu, L. W. Fu, S. Kaiser, H. Schweizer, and H. Giessen, Adv. Mater. **20**, 3859 (2008).
[18] Z. G. Dong, H. Liu, T. Li, Z. H. Zhu, S. M. Wang, J. X. Cao, S. N. Zhu, and X. Zhang, Appl. Phys. Lett. **96**, 044104 (2010).
[19] J. M. Hao, Y. Yuan, L. X. Ran, T. Jiang, J. A. Kong, C. T. Chan, and L. Zhou, Phys. Rev. Lett. **99**, 063908 (2007).
[20] T. Li, H. Liu, F. M. Wang, Z. G. Dong, S. N. Zhu, and X. Zhang, Opt. Express **14**, 11155 (2006).
[21] The discrepancies in small s/p region are considered arising from the coupling between the cavity and pure plasmonic modes, which lead to avoiding crosses in mode diagrams. The detailed analyses of such coupling effects will be discussed elsewhere.